Supplementary material

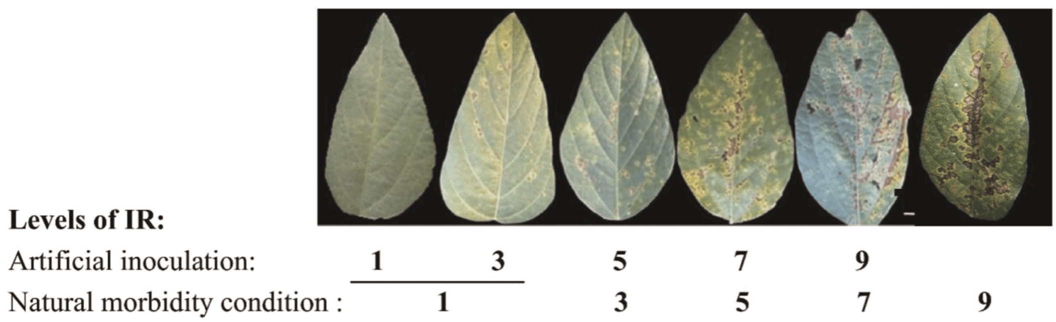

Figure S1: Bacterial pustule disease symptoms scaled by the disease spot numbers. The bacterial pustule resistance performance of soybean plants were assessed as five levels [10].

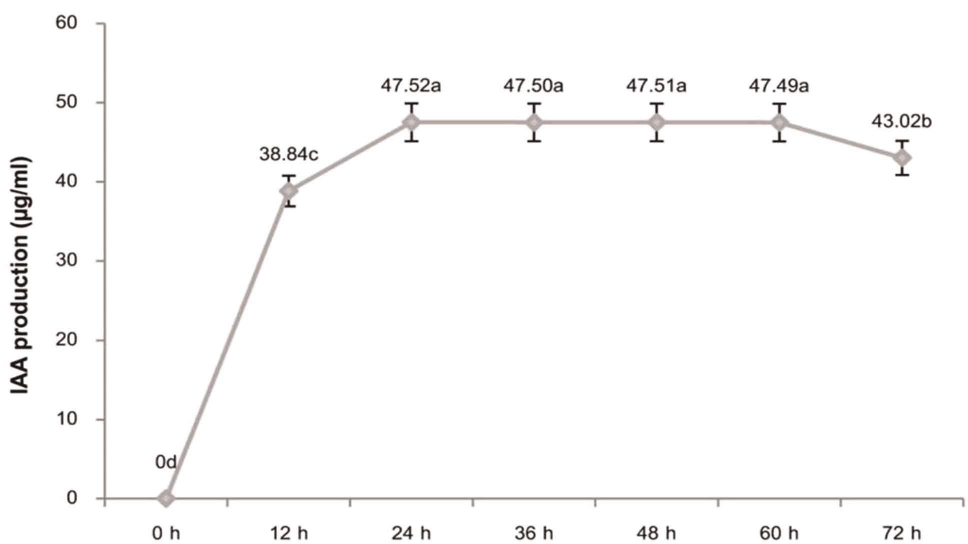

Figure S2: PR-HPLC profile of indole-3-acetic acid (IAA) produced by *Pseudomonas fluorescens* SP007s in NGB medium at 12, 24, 36, 48, 60, and 72 h. The HPLC setup consists of a Sunfire column with dimensions of 4.6 × 150 nm and a particle size of 5 μm. The mobile phase used is a mixture of 26% V/V acetonitrile and water at 4 pH. The flow rate is set at 1.2 ml/min, and the injection volume is 10 μl. The IAA analytical standard, obtained from Sigma-Aldrich, USA, was used as the standard for analysis. Means in the graph followed by different letters are significantly different according to DMRT at $p \leq 0.05$.

Table S1: The spectra band assignments of the FTIR vibration peaks (cm^{-1})

Wavenumber (cm^{-1})	Peak name	Chemical composition	References
3,000–2,800	C–H stretching	CH_2 asymmetrical and symmetrical stretching phospholipid	[1]
1,740–1,700	C═O esters	Lignin and hemicellulose, pectin	[2]
1,700–1,600	C═O vibrational stretch, 10% N–H stretch and protein, contribution from C–N stretch absorptions	Amide I, α-helical protein secondary structures	[2–4]
1,600–1,500	N–H bending and C–N stretching of protein (N–H bend (60%), C–N stretch (40%)	Amide II, α-helical and β-sheet protein secondary structures	[5,6]
1,515, 1,517	C + C aromatic ring from lignin	Lignin	[7]
1,470–1,350	C–H bending from CH_2 and CH_3 symmetric bending	Unsaturated fatty, phospholipids	[1]
1,300–1,200	C–O stretching of hemicellulose and lignin	Hemicellulose and lignin	[8]
1,145, 1,114, 1,060	C–O, C–C, C–O–C	Polysaccharides	[2,9]

Table S2: Efficacy of *Pseudomonas fluorescens* SP007s on plant growth promotion of soybean in greenhouse conditions

Treatments	Stem height (cm)						Root length (cm)					
	7 dps	14 dps	21 dps	28 dps	35 dps	42 dps	7 dps	14 dps	21 dps	28 dps	35 dps	42 dps
SP007s	4.20a	9.30a	17.30a	26.30a	32.40a	38.60a	5.60a	8.70a	12.00a	15.80a	17.80a	19.80a
Salicylic acid	3.10b	8.20b	15.80b	23.40b	28.20b	31.50b	5.70a	8.40a	12.12a	15.20a	16.10a	17.00b
Copper hydroxide 77% WP	2.50c	6.50c	15.80b	20.80c	23.00c	26.80c	3.98c	6.11c	10.01b	12.80b	14.00ab	14.58c
Water-mock	3.51b	6.30c	15.50b	22.40b	25.90c	27.40c	4.50b	7.76b	11.76a	14.15a	15.11b	16.90b

[1/]Soybean seeds were soaked in 50 mL of each treatment solution, germinated on wet filter paper in the dark, and planted in 30 cm diameter pots containing sterile soil and organic fertilizer. [2/]Stem height and root length were measure at 7-day intervals. Values are presented as the mean of four replicates, twenty-five seeds per replication. Means in the graph followed by different letters is a are significantly different according to DMRT at $p \leq 0.05$.

References

[1] Rohman A, Che Man YB. The optimization of FTIR spectroscopy combined with partial least square for analysis of animal fats in quartenary mixtures. Spectroscopy. 2011;25:825121. doi: 10.3233/SPE-2011-0500.

[2] Murray-Wijelath J, Lyman DJ, Wijelath ES. Vascular graft healing. III. FTIR analysis of ePTFE graft samples from implanted bigrafts. J Biomed Mater Res B Appl Biomater. 2004;70:223–32. doi: 10.1002/jbm.b.30044.

[3] Wang Q, He H, Li B, Lin H, Zhang Y, Zhang J, et al. UV–Vis and ATR–FTIR spectroscopic investigations of postmortem interval based on the changes in rabbit plasma. PLoS One. 2017;12:e0182161. doi: 10.1371/journal.pone.0182161.

[4] Baker MJ, Gazi E, Brown MD, Shanks JH, Gardner P, Clarke NW. FTIR-based spectroscopic analysis in the identification of clinically aggressive prostate cancer. Br J Cancer. 2008;99:1859–66. doi: 10.1038/sj.bjc.6604753.

[5] Thepbandit W, Buensanteai N, Thumanu K, Siriwong S, Le Thanh T, Athinuwat D. Salicylic acid elicitor inhibiting *Xanthomonas oryzae* growth, motility, biofilm, polysaccharides production, and biochemical components during pathogenesis on rice. Chiang Mai J Sci. 2021;48:341–53.

[6] He Z, Liu Y, Kim HJ, Tewolde H, Zhang H. Fourier transform infrared spectral features of plant biomass components during cotton organ development and their biological implications. J Cotton Res. 2022;5:11. doi: 10.1186/s42397-022-00117-8.

[7] Md Salim R, Asik J, Sarjadi MS. Chemical functional groups of extractives, cellulose and lignin extracted from native *Leucaena leucocephala* bark. Wood Sci Technol. 2021;55:295–313. doi: 10.1007/s00226-020-01258-2.

[8] Parihar A, Vongsvivut J, Bhattacharya S. Synchrotron-based infrared spectroscopic insights on thermo-catalytic conversion of cellulosic feedstock to levoglucosenone and furans. ACS Omega. 2019;4:8747–57. doi: 10.1021/acsomega.8b03681.
[9] Chukanov NV, Chervonnyi AD. IR spectra of minerals and related compounds, and reference samples' data. In: Chukanov NV, Chervonnyi AD, editors.. Infrared spectroscopy of minerals and related compounds. Cham: Springer International Publishing; 2016. p. 51–1047.
[10] Zhao F, Cheng W, Wang Y, Gao X, Huang D, Kong J, et al. Identification of novel genomic regions for Bacterial Leaf Pustule (BLP) resistance in soybean (*Glycine max* L.) via integrating linkage mapping and association analysis. Int J Mol Sci. 2022;23:2113.